

Macroscopic Evidence of Carbon Nanotube Bundles

Electronic Properties

M. Salvato^{a,b}, M. Cirillo^a, M. Lucci^a, S. Orlanducci^c, I. Ottaviani^a, M.L. Terranova^c, and F. Toschi^c

^{a)} *Dipartimento di Fisica and MINAS Laboratory, Università di Roma “Tor Vergata”, I- 00133 Roma*

^{b)} *Laboratorio Regionale “Super Mat” CNR-INFN, I-84081, Baronissi, Italy*

^{c)} *Dipartimento di Scienze e Tecnologie Chimiche and MINAS Laboratory, Università di Roma “Tor Vergata”, I- 00133 Roma*

Abstract

We report on experiments conducted on single walled carbon nanotube bundles aligned in chains and connected through a natural contact barrier. Exploring the current-voltage characteristics in the (5-300)K temperature range we find evidence of voltage gaps whose value, in the (50mV-2.5V) interval, is consistent with microscopic results. We also show evidence of Coulomb Blockade steps and Van Hove singularities generated respectively by the metallic and the semiconducting components both present inside the nanotube bundles. Connecting two electrodes separated by a distance of 100 μ m by chains of bundles we observe gap sum voltages that are consistent with a circuit model. The measured gap dependency upon temperature is also analyzed in terms of a potential sensor application.

The interest for the physical properties of carbon nanotubes (CNT) systems has much grown after the fabrication of transistors and diodes based on metal or semiconducting CNT [1]. Recently, field effect transistors consisting of a single nanotube bundle showing negative differential conductance (NDC) at room temperature were theoretically predicted [2] and fabricated [3]. In the present paper we report on transport measurements performed on bundles containing semiconducting and metallic single wall (SW)CNT aligned along the bias current direction. We observe several effects in the current-voltage characteristics of the devices (energy gap, single electron tunneling and Van Hove singularities) which are consistent with microscopic observations and can be justified by the presence, inside the bundles, of metallic and semiconducting SWCNT.

Bundles of SWCNT [4] were deposited on insulating SiO₂ substrates where metallic Al contacts had been previously patterned with the four lead configuration shown in the inset of Fig.1a. The distance between the main voltage electrodes is $100\mu m$ while the minimum distance in the corners (see the area inside the white rectangle) is $5\mu m$. The bundles were aligned along the arrow direction by a dielectrophoretic technique described elsewhere [5]. The contact geometry allows selecting two different probing configurations referred to as NTPR1 and NTPR2 (NanoTubes Probe 1/2). For the NTPR1 the electrodes P1 and P2 are used as current probes and the electrodes P3 and P6 as voltage probes. For the NTPR2, electrodes P1 and P5 are used for the current injection while P3 and P4 are used as voltage probes. Scanning Electron Microscopy (SEM) revealed that the length of each bundle ranges between $2\mu m$ and $3\mu m$ and that their diameter is typically of the order of $100nm$. Thus, we found that for the NTPR1 configuration a chain formed by few bundles would be connecting the voltage electrodes of the corners just as shown in Fig.1a where we see the “minimal” chain formed only by two bundles. Instead, for NTPR2 roughly 40 equally spaced parallel chains, each consisting of about 40 aligned bundles, cover the $100\mu m$ distance between the voltage electrodes P3 and P4. For all the samples, the SWCNT contained inside the bundles have nominal diameters and length $D=2nm$ and $L=1\mu m$ respectively. The contact between the CNT inside each bundle, between the different bundles and with the electrodes is supposed to be due to the action of

van der Waals forces between the graphenic surfaces with a consequent potential barrier formation[6].

Transport measurements have been performed in a high vacuum cryocooler equipped for four probe resistance vs. temperature ($R-T$) and current-voltage ($I-V$) measurements in the range ($5K-300K$). Fig.1b shows the $I-V$ characteristics at $T=5K$ acquired using a current power supply. A step $\Delta V \cong 50mV$ in the voltage is observed at $V_0 \cong 70mV$ when the current passes the value $I_0 \cong 0.13\mu A$. This voltage step ΔV is caused by a sharp decrease of the electrical conductance and it is reminiscent of that observed in current biased semiconducting tunnel diodes showing NDC phenomena[7] and related to the misalignment of the electronic bands positioned at different sides of the junction.

In order to better investigate the observed discontinuity we voltage biased our samples obtaining the $I-V$ characteristic shown in Fig.2a. Voltage biasing is suitable in $I-V$ spectroscopic measurements when band edge effects have to be considered because of the gradual variation of electronic bands with respect to the Fermi level. Both the curves of Fig. 1b and Fig. 2a were highly symmetric indicating that the effect of the substrate and the metallic contacts on the electronic band structure of the bundles is negligible. Moreover, both the curves present discontinuity in the same voltage range. When the nanotube bundles junctions are voltage biased, the step in Fig. 1b is replaced by a singularity due to an increase of the conductivity and hysteresis is present. Both the singularities and the corresponding hysteresis are also present at higher voltage as shown in Fig. 2a in the V-shaped curve where the conductance, as calculated by the $I-V$ measurement at $T=5K$, is shown. These singularities are found to arise at $V_1 \cong \pm 105mV$, $V_2 \cong \pm 210mV$, $V_3 \cong \pm 420mV$. These values are in the ratio $1:2:4$ which is the one predicted for Van Hove Singularities (VHS) in the electronic band structure of semiconducting SWCNT [8] and found experimentally by scanning tunnel spectroscopy [9]. The presence of semiconducting SWCNT inside the bundles suggests that a band structure is formed in each bundle and that electrons tunnel the potential barrier between two bundles at fixed values of the voltage drop.

The experimental values found for VHS in our case are lower than those predicted theoretically for isolated SWCNT which give for the first VHS the value $\varepsilon_1 = \pm \gamma_0 a_{cc} / D = 170 \text{ mV}$ where $\gamma_0 = 2.5 \text{ mV}$ is the nearest-neighbor overlap integral of graphite sheet, $a_{cc} = 0.14 \text{ nm}$ is the distance between two adjacent carbon atoms and $D = 2 \text{ nm}$ is the diameter of the tubes. This quantitative discrepancy can be explained considering that the theoretical value is obtained for isolated semiconducting SWCNT and does not take into account the effects of the tubes curvature, the surface contact between different SWCNT inside the bundles and their finite length. Experimental studies have widely demonstrated that the energy gap in semiconducting SWCNT is strongly affected by these effects [10] and its value can be even much less than the ideal value $\Delta E = 2\varepsilon_1$.

Fig.2b shows an expanded area of Fig.2a where the low bias part of the I - V characteristic is shown. The conductance increases in steps whose width depends on the voltage; these steps, however, disappear when the temperature raises above 15 K . This behavior is typical in Luttinger Liquid (LL) where electrons interact each others giving rise to Coulomb Blockade effects [11,12]. To confirm the LL regime, the temperature dependence of the measured electrical conductance $G = I/R$ is reported in the inset of Fig.2b in double logarithmic scale. The line is a fit to the data assuming a power law dependence $G = T^\alpha$ obtained for $\alpha = 0.68$. A power law dependence is expected in the case of LL behavior where the interaction between electrons is quantified by the value of the LL parameter g which is as low as the electronic interaction is strong [12]. The value of α depends on g and on the given contact geometry. In our case, this dependence is $\alpha = (1/g + g - 2)/8$ which gives $g = 0.14 \ll 1$ confirming a strong electrons interaction and the possibility of Coulomb Blockade effects.

Fig.2c shows the width of the conductance steps dV , observed in Fig.2b, as a function of the voltage value corresponding to each step discontinuity. The figure shows a decrease of dV with voltage up to 65 mV , followed by an alternate behavior between $dV = 2 \text{ mV}$ and $dV = 4 \text{ mV}$. The data are reported up to a voltage of 100 mV , corresponding to the increase in the conductance caused by

VHS where the steps are not distinguishable anymore. The alternate values of dV correspond to the addition energy required to add one electron to a state of N electrons as schematically shown in the inset of Fig.2c. Following the Constant Interaction (CI) model developed for quantum dots[13] and successfully applied in the case of SWCNT[14], the electrons in the metallic nanotubes can be considered as independent particles in a box of length L equal to the CNT length. This approximation gives an average energy level spacing for the electrons[11,14] of $E=hv_F/2L=1.7meV$ where h is the Planck constant, $v_F=8.1\cdot 10^5$ m/s is the Fermi velocity and $L=1\mu m$. Moreover, the electrons transport a Coulomb energy given by $U=e^2/2C\cong 2meV$ if a tube capacity $C\cong 4\cdot 10^{-17}$ F[15] is considered (here e is the electron charge). The values reported for dV in Fig.2c are in good agreement with these data and describe the transport mechanism between the metallic nanotubes[14]. The maximum value $U+E=4mV$ corresponds to a thermal energy $k_B T$ with $T=16K$ which means that conductance steps can be revealed only for $T<16K$ which is consistent with our measurements.

We shall see now that measurements of the aligned bundles in the NTPR2 configuration can provide further evidence for the metallic and semiconductor properties that we have investigated so far. Fig. 3a shows I - V curves obtained at different temperatures in the NTPR2 configuration; we put in the upper left corner of the figure an inset with two SEM images of two chains of bundles contacting the pads and a zoom taken in the central area between the pads P3 and P4 (see inset of Fig.1a). The inset in the lower right corner shows instead an I - V characteristic of the same sample in the NTPR1 configuration at $T=7K$: here we can see that $V_0\cong 70mV$, $I_0\cong 0.8\mu A$ and $\Delta V\cong 50mV$. Comparing the two configurations (NTPR1 and NTPR2) we observe that in both cases a voltage switch occurs for bias current above a peak value I_0 ; increasing the current above this value the transport is governed by thermal assisted tunneling [16]. Also, the metallic resistance in the low current bias region for NTPR2 is $R\cong 2k\Omega$ which is much lower than that observed for NTPR1. The amplitude of the voltage discontinuity ΔV and the current I_0 (compared at the same temperatures) in the NTPR2 configuration are much higher than those of NTPR1. The larger values of I_0 and ΔV

allow measuring their temperature dependencies with “safe” uncertainty margins as shown in Fig.3b and Fig.3c respectively. The voltage amplitude ΔV of the discontinuity traced in Fig. 3a decreases with the temperature (see Fig. 3b) according to an exponential law $\exp(-T/T_0)$ with $T_0=470K$; the continuous line in Fig.3c shows the functional dependency of the Anderson’s emission model [17] describing the carrier transport across heterojunctions. Both the dependencies of Fig.3b and Fig.3c indicate that we are dealing with a process in which electrons overcome a barrier energy under the action of an external field [7,17,18].

Based on the data and analysis made in the last paragraph, the possible transport mechanism in the samples can be explained following the sketches in the insets of Fig.3b and Fig.3c. At low bias current, the charge transport takes place by tunneling both through metallic and semiconducting SWCNT bundles separated by the junction barriers. In this regime, voltage drop increases linearly with the current and the semiconducting bands start to be misaligned (follow here inset of Fig. 3b from left to right). When $V=V_0$, (rightmost picture) the tunneling through semiconducting SWCNT stops because of the complete misalignment of the conduction bands and the current tunnels only through the metallic SWCNT: this phenomenon causes a sharp decrease of the electrical conductance. In this scenario, $V_0 \cong 70mV$ gives the bandwidth and $\Delta V \cong 50mV$ corresponds to the gap energy in the semiconducting SWCNT. The reason for the lower values of the resistance below I_0 and for the larger values of ΔV in NTPR2 configuration with respect to the NTPR1 has to be ascribed to the fact that there are several chains of bundles carrying current in parallel while the voltages are measured across the whole length of the parallel chains (in the inset of Fig.3c every cross represents a junction between bundles). Thus, in the case of NTPR2, the values of ΔV can be interpreted as due to sum of the individual voltage drops across the junctions deposited in parallel between the two voltage electrodes which are spaced $100\mu m$ away. For the measured samples the number of junctions is of the order of 40 and a voltage step $\Delta V=40 \times 50mV=2V$ is expected at $T=7K$. The measured value of $2.5V$ at $T=7K$ in Fig.3a is higher but provides the expected order of

magnitude. Moreover, for the 40 parallel bundles chains of the NTPR2 bias configuration, the current value $I_0=30\mu A$ corresponds to a peak current of $30\mu A/40=0.75\mu A$ in each bundle chain which is in good agreement with the results shown in the inset of Fig.3a.

The large voltage discontinuities observed offer an interesting applied physics counterpart. The time required for electrons to transit between the electrodes placed $5\mu m$ apart in NTPR1 can be roughly estimated by summing the time to move along two nanotubes of $2\mu m$ at the Fermi velocity $v_F=8.1\cdot 10^5 m/s$ and the tunneling time given by the uncertainty relation $\tau = \hbar/e\Delta V$ where \hbar is the Planck constant divided by 2π , e the electron charge and $\Delta V \cong 50mV$. The calculation gives $\tau \cong 2\cdot 10^{-12}s$ as switching time which is of the same order of the fastest semiconducting based switching devices. In Fig.4 the R vs. T curves are reported for the NTPR2 configuration for three different values of the d.c. bias current I_{bias} . When the $I_{bias} = 50\mu A$, well above the I_0 range shown in Fig.3b, a typical semiconducting behavior is observed [16]. When $I_{bias}=20\mu A$ is below of I_0 an ohmic behavior is recorded. Instead, when $I_{bias}=30\mu A$ is close to I_0 , a large step in the resistance is observed. The step in the resistance and the temperature value where this step is observed depend on the bias current used and we found that the dependence of the switchings on the specific current value was highly reproducible. The contact barriers were generated just by the overlapping of the bundles during alignment and no further processing was required; thus, the switching currents of the devices could just be tuned by increasing the density of bundles in the fabrication procedure and the switching voltages could be tuned by adequately selecting the length between the electrodes. This relative ease in the fabrication process and the “a priori” determination of the characteristics of the samples are particularly stimulating in view of device applications.

We are grateful to Prof. C. Attanasio at University of Salerno (Italy) for helpful discussions and comments.

References

- [1] S.J. Tans et al., Nature **393**, 49(1998); M. Rinkio et al., Nano Letters **9**, 643(2009).
- [2] S. Maksimenko and G. Y. Slepyan, Phys. Rev. Lett. **84**, 362(2000).
- [3] G. Buchs et al., Appl. Phys. Lett. **93**, 73115(2008); M. Dragoman et al., Appl. Phys. Lett. **93**, 43117(2008).
- [4] B. Mateusz et al., Adv. Mater.**17**,1186(2005).
- [5] M.L. Terranova et al., J.Phys.D: Condensed Matter **19**, 2255004 (2007).
- [6] J.C. Charlier, X. Blasé, S. Roche, Rev. Mod. Phys. **79**, 677(2007).
- [7] D.K. Ferry and S.M. Goodnik, *Transport in nanostructures*, Cambridge University Press (2001); R.A. Davies, M.J. Kelly, and T.M. Kerr, Phys. Rev. Lett. **55**, 1114(1985).
- [8]C.T. White, J.W. Mintmire, Nature **394**, 29(1998).
- [9] L.C. Venema et al., Phys. Rev. **B62**, 5238(2000)
- [10] D.L. Carroll et al., Phys. Rev. Lett. **78**, 2811(1997)
- [11] M. Bockrath et al., Science **275**, 1922(1997).
- [12] A. Bachtold et al., Phys. Rev. Lett. **87**, 166801(2001); M. Bochrath et al. Nature **397**, 598(1999).
- [13] L.P. Kouwenhoven, D.G. Augustin, and S. Tarucha, Rep. Prog. Phys. **64**, 701(2001)
- [14] D.H. Cobden, J. Nygard, Phys. Rev. Lett. **89**, 046803(2002); P.J. Herrero et al., Nature **429**, 389(2004).
- [15] L. C. Venema et al., Science **283**, 52(1999)
- [16] P. Sheng, Phys. Rev. **B21**, 2180 (1980); M. Salvato et al., Phys. Rev. Lett. **101**, 246804(2008); W. Ren et al., Phys. Rev. **B78**, 195404 (2008); H. Xie and P. Sheng, **B79**, 165419 (2009).
- [17] L.W. Liu et al., Phys. Rev. **B71**, 155424(2005).
- [18] G. Margaritondo, *Electronic Structure of Semiconductor Heterojunctions*, Ed. Kluwer, Boston (1988).

Figure Captions

Fig.1 a) Scanning electron microscopy of two aligned bundles between voltage electrodes. The arrow shows the junction between the bundles. The inset shows an optical photograph of a sample; b) typical current-voltage characteristics (current bias) of a junction formed at the contact between two bundles.

Fig. 2. a) I - V characteristics at $T=5K$ using voltage bias; the V-shaped curve shows the conductance vs. voltage calculated from the I - V curve; b) zoom of the metallic portion of the (metallic) conductance plot showing VHS and hysteresis. The arrows indicate the direction of the voltage sweep. dV indicates the voltage step as reported in Fig.3b. Inset: Double logarithmic plot of conductance vs. temperature measurement of a SWCNT sample. The line is a fit to the data using the expression $G=T^\alpha$ obtained with $\alpha=0.66$; b) Voltage step measured in Fig.3a as a function of the voltage. Inset: sketch of the charge transport in CI model.

Fig. 3. a) Temperature dependence of the current-voltage characteristics (current bias) in the NTPR2 configuration. The left-top inset shows typical SEM images with two bundles departing from a contact and a zoom (white framed) in the central area between the electrodes. The white ruler length is $0.5 \mu m$. The right-low inset shows the I - V curve of the same sample in the NTPR1 configuration; b) dependence of the maximum current I_0 upon the temperature. The inset is a sketch for the conduction process ; c) the dependence of the voltage gap in a) upon the temperature. The inset is the electrical model consisting of parallel chains of series connections of bundles junctions.

Fig. 4. The biasing diagrams for a temperature sensor based on the phenomenon measured in Fig. 3a. When the bundles are biased at about the switching current I_0 an abrupt change in their resistance can be caused by the temperature.

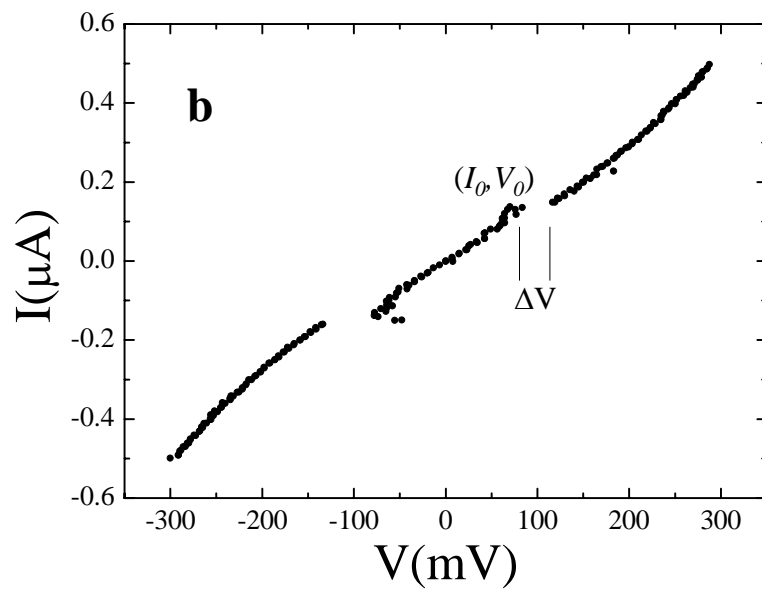
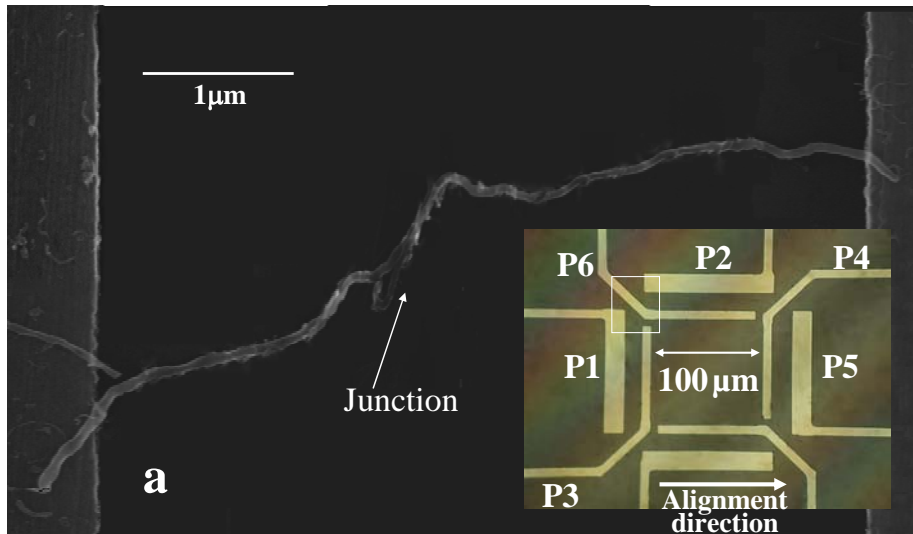


Figure 1, M. Salvato et al.

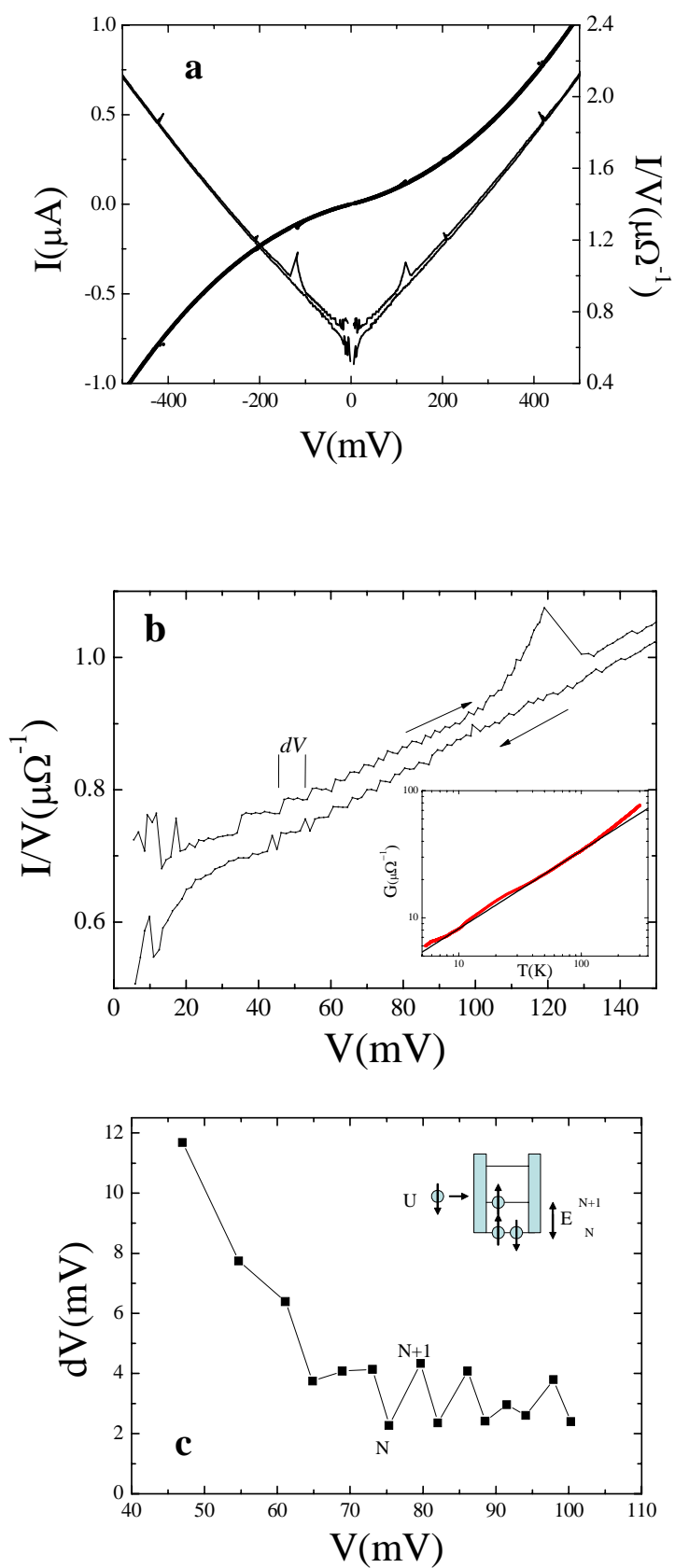


Figure2, M. Salvato et al.

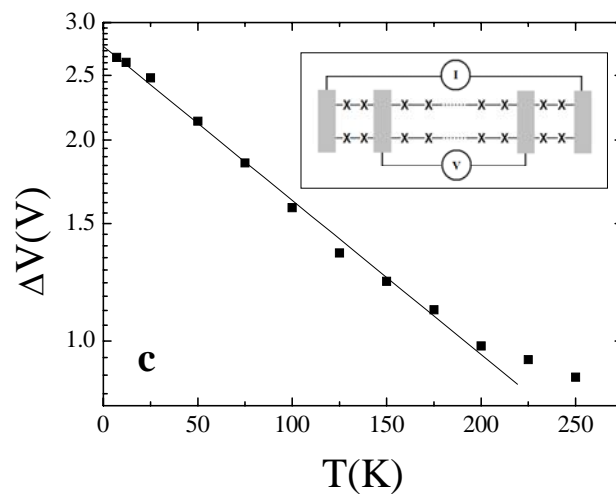
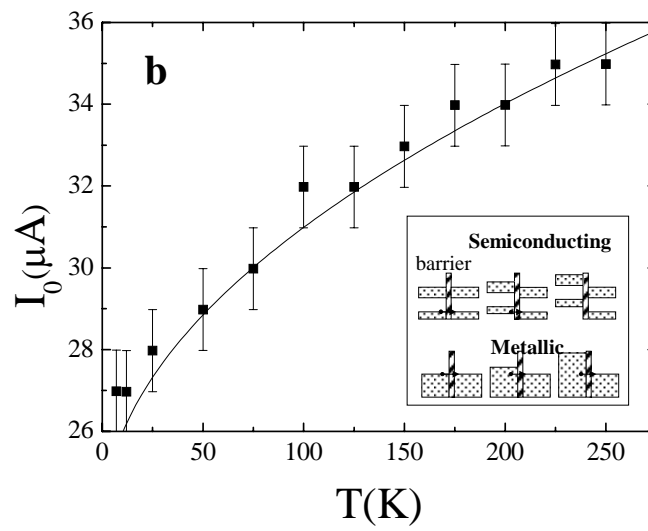
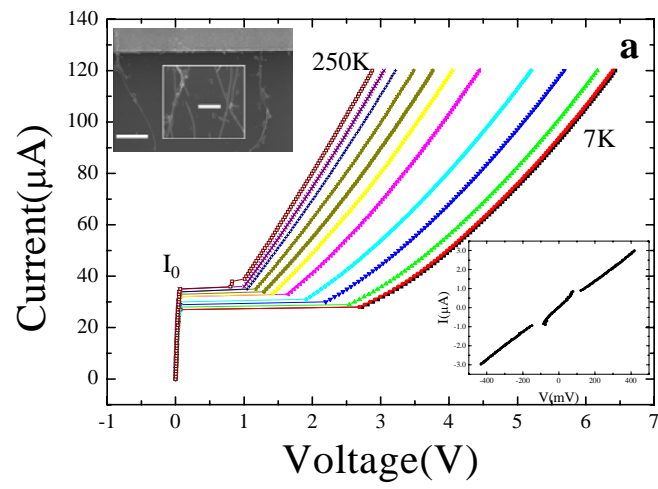


Figure 3, M. Salvato et al.

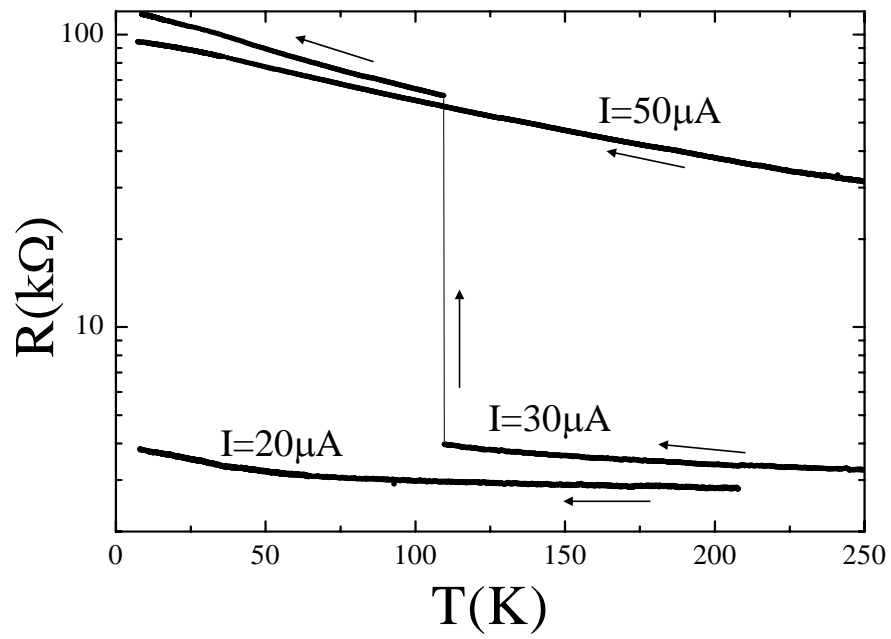


Figure 4, M. Salvato et al.